Contents lists available at Science-Gate

International Journal of Advanced and Applied Sciences

Journal homepage: http://www.science-gate.com/IJAAS.html

Modeling of parasitic effects in multi-rotor hybrid aircrafts: Part-I

Ali Shahbaz Haider *, Riaz Ali, Qamar Aftab, Muhammad Asim, Tayyab Akram

Department of Electrical Engineering, COMSATS Institute of IT, Wah, Pakistan

ARTICLE INFO

Article history:
Received 20 May 2016
Received in revised form
7 July 2016
Accepted 8 July 2016

Keywords:
Effects
Hybrid aircrafts
VTOL
T-Copter
Parasitic presession
Gyroscopic moment

ABSTRACT

This article presents the detailed modeling and analysis of the precession and the gyroscopic parasitic effects that creep into the dynamics of multi-rotor hybrid aircraft during transient and steady state flight conditions. The term "parasitic" collectively refer to undesirable effects such as coriolis, centripetal and centrifugal acceleration; gyroscopic moments, rotor tilt reaction moment, inertial counter torques, frictional moments and air drag moments, precession moments etc. These effects are the major source of nonlinearity and coupling in the dynamics of aircraft. The hybrid aircraft combines the features of the hovercraft and the wing craft. A Tee configuration tri-rotor hybrid aircraft with the tilt-rotor and the tilt-wing mechanism would be taken into account and the parasitic precession moments and the gyroscopic moments would be modeled for it in the detail, in a way that this analysis could easily be extended to multi-rotor hybrid craft with the different number of rotors in any given configuration.

1. Introduction

The multi-rotor hybrid aircraft is a flying platform with more than one motor-propeller assembly and it combines the flight features of the hovercraft and the wing aircraft. It can vertically take off and land (VTOL) and can hover in the air like helicopters (Haider and Sajjad, 2012). To track flight trajectory or to hover, the hybrid crafts can change the configuration of the rotors using a tilt-wing mechanism, effectively transforming them from the wing crafts configuration to the hovercraft configuration and vice versa (Partovi et al., 2011). They have many civilian and military applications, for example, surveillance, helicopter path inspection, disaster monitoring and land sliding observation, data and image acquisition of targets etc. (Kendoul et al., 2005). There is a boom in the development of the mini flying robots because of their immense significance and applications. A hybrid aircraft has a lot of benefits over the airplane and the helicopter; it does not have swash plate and does not need any runway. It can hover like a helicopter and it has the flight capabilities of the wing aircraft. A hybrid aircraft uses propellers that have fixed pitch, making it much economical and controllable (Etkin, 1959). It has the advantage over tail-sitter aircraft owing to the literal position at the take-off, landing and in the hover mode, rather than the vertical position in the case of tail-sitters, which poses problems for the pilot and the payload placement. A hybrid aircraft is available in various configurations (Haider and Sajjad, 2012) and designs e.g. star, delta, mesh, cross structures (Goel et al., 2009). One of the most famous configurations is the Tee structure, known as T-Copter (Cruz et al., 2008). It is a challenging system to be modeled and controlled. Tiltrotor is a mechanism, which is used in most of the T-Copter to control the yaw. The objective of our research is to develop VTOL based hybrid aircraft (Zhang and Brandt, 1999) however; the multiple rotor-propeller sets produce complicated dynamic effects during hover as well as during maneuvers like roll, pitch and yaw. These effects result in the nonlinearities in the dynamics of the craft as well as introducing cross coupling in the dynamics (Johnson, 2012). These effects are called "parasitic" because they are the byproduct of the desired maneuvers during hover and flight. A sound understanding of these effects may enable us to mitigate or counterbalance them by appropriate structural configuration selection and design modifications (Leishman, 2006). This research paper comprises of our work corresponding to the detailed analysis of the parasitic precession moments and the gyroscopic moments that are generated in the T-Copter hybrid aircraft during its typical maneuvers. Some of these

* Corresponding Author.
Email Address: alishahbaz@ciitwah.edu.pk (A.S. Haider)
http://dx.doi.org/10.21833/ijaas.2016.07.003

effects appear during transients in roll, pitch and yaw, while some may appear even during the steady state hover. This is the part I of the two-part work. In this part, the precession and the gyroscopic parasitic effects will be taken into considerations while the other effects will be discussed in part II of this article.

The organization of the paper is as follows: Section 2 describes the overview of the hybrid craft hardware and its dynamics in general. Section 3 describes the identification of terms that account for the parasitic effects and presents the modeling of these effects. Section 4 deals with the modification of general dynamics of the hybrid aircraft to incorporate the effects of the parasitics that have been modeled in Section 3. Section 5 presents the discussion and conclusion and future task.

2. Overview of hardware and dynamics

2.1. Symbols and terminology

Various symbols and the terms that have been used to describe the dynamics of the T-copter are enlisted below:

$\mathbb{R}$=Real Space.
ϕ =roll, counter clockwise positive.
θ =Pitch, counter clockwise positive.
ψ =yaw, counter clockwise positive.
$\boldsymbol{\eta}(\phi,\theta,\psi) \in \mathbb{R}^3$ =Angular displacement vector of the craft.
M =mass of each rotor.
ω_i =angular velocity of the i^{th} rotor.
m =mass of entire hovercraft structure.
$\mathbf{I} \in \mathbb{R}^{3\times3}$ =Pseudo inertial matrix.
$\mathbf{R} \in \mathbb{R}^{3\times3}$ =Rotational matrix.
$\boldsymbol{\beta}(E_1,E_2,E_3)$ =Body frame of reference.
$\boldsymbol{\Lambda}(E_x,E_y,E_z)$ =Inertial frame of reference.
$C.G.$ =centre of gravity of the hovercraft body.
ω_b = angular velocity of craft body around $C.G.$
$\boldsymbol{\xi}(x,y,z) \in \mathbb{R}^3$ =position of the $C.G.$ in Λ.
l_j =lengths of the respective sides of the hovercraft body.
r_j = distance of a point j from the given axes of rotation.
$\mathbf{F} \in \mathbb{R}^3$ =force vector in β.
$\boldsymbol{\tau} \in \mathbb{R}^3$ =torque vector.
$\mathbf{F_i}$ =Force vector of the i^{th} rotor.
$\aleph \in \mathbb{R}^3$ =parasitic moment term in the system dynamics.
$\wp \in \mathbb{R}^3$ =parasitic acceleration term in the system dynamics.

2.2. System hardware

The target system hardware is a tri-rotor hybrid aircraft as shown in Fig. 1. It can be considered a T-copter rotorcraft with two main rotors and one tail rotor.

The tail rotor has a tilt rotor mechanism as shown in Fig. 2, which comprises of a servo motor that tilts a shaft coupled to the tail rotor, hence controlling the angle of inclination of the tail rotor. This mechanism controls the yaw and compensates some of the parasitic effects, as it will be explained in the further sections.

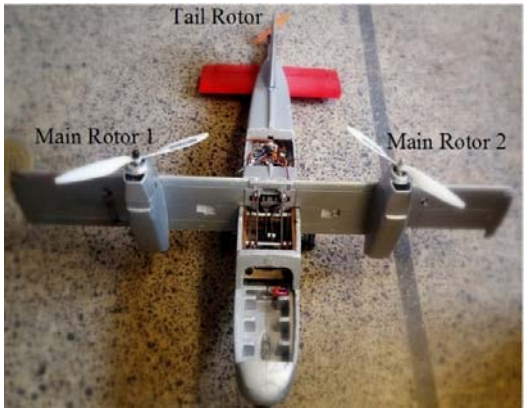

Fig. 1: The hybrid craft hardware

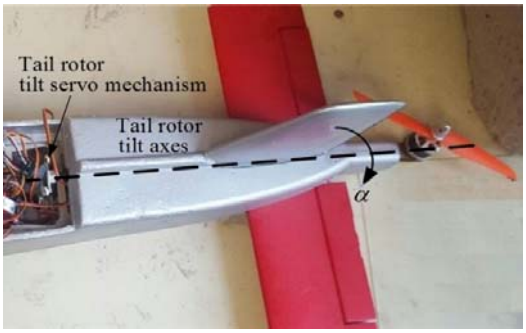

Fig. 2: The tail rotor tilts mechanism

The tilt wing mechanism is shown in Fig. 3. It transforms the aircraft structure form the hover mode to the flight mode and vice versa, using a servo mechanism similar to the tilt rotor mechanism.

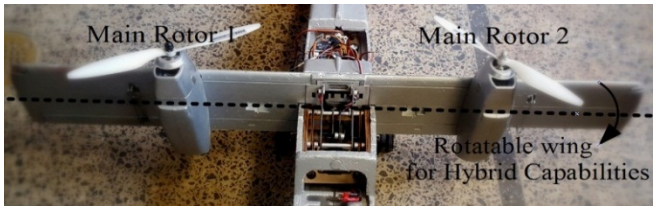

Fig. 3: The tail wing mechanism

A simplified T-Copter structure for the hardware modelling is shown in Fig. 4. The frames of references and reference directions of rotations of various rotors are also shown in Fig. 4. It is worth noting that the two main rotors rotate in opposite directions to cancel some of the parasitic effects as explained in further sections. The tilt rotor mechanism for the tail rotor is explained schematically in Fig. 5.

The Newton-Euler's equations govern the dynamics of any general aircraft (Haider and Sajjad , 2012). These equations describe the dynamics of the body of the aircraft in the inertial frame of reference and these equations are given by:

$$m\frac{d^2\xi}{dt^2} = \mathrm{RF} - mg\mathrm{E_z} + \wp(\omega_j, r_i, \xi, \eta) \qquad (1)$$

$$I\frac{d^2\eta}{dt^2} = \tau + \aleph(\omega_j, l_k, r_i, \eta)$$

where $E_z = [0 \quad 0 \quad 1]^T$.

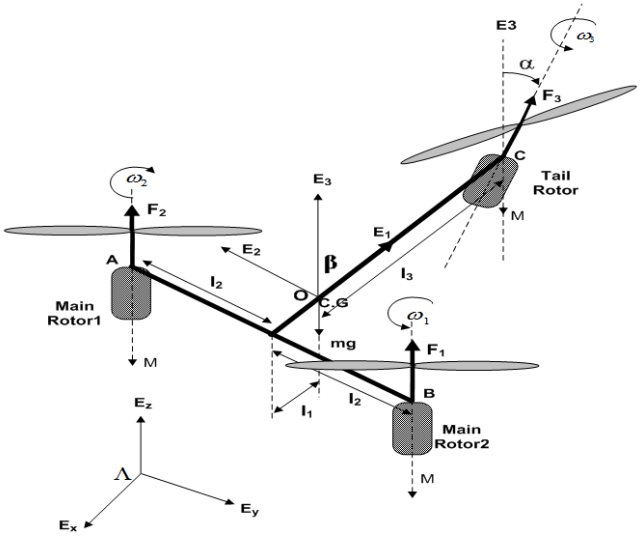

Fig. 4: Simplified T-Copter Structure for the system modeling

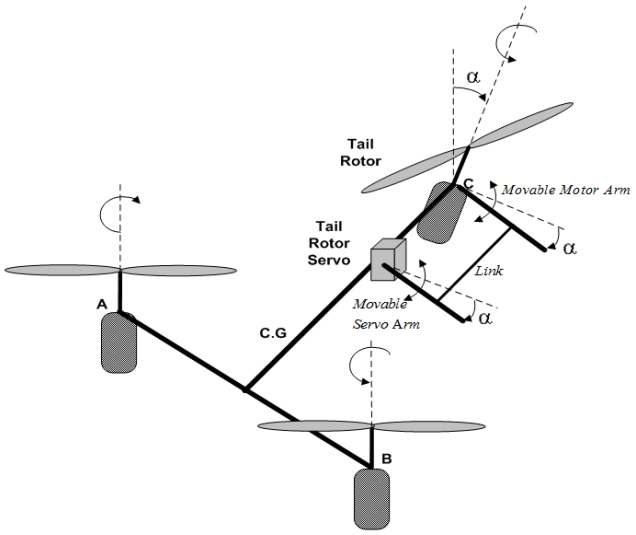

Fig. 5: The Servo mechanism to adjust the tail rotor tilt angle α

3. Parasitic effects in aircraft dynamics

The terms in the vectors $\wp$ and the vector $\aleph$ in Eq.1 correspond to the parasitic accelerations and the parasitic moments respectively. Various parasitic effects can be categorized as follows:

1. The precession moments.
2. The gyroscopic moments.
3. The air drag moments.
4. The angular acceleration effects.
5. Reaction moments.
6. Frictional moments.

The parasitic moment term $\aleph$ can be decomposed into three terms for this research paper as given by Eq. 2.

$$\aleph = \aleph_p + \aleph_g + \aleph_m \qquad (2)$$

where,

1. $\aleph_p$=Parasitic precession moments.
2. $\aleph_g$=Parasitic gyroscopic moment.
3. $\aleph_m$=Parasitics other than $\aleph_p$ and $\aleph_g$.

This research article is concerned with the detailed evaluations of precession and gyroscopic moments. The effects included in the term $\aleph_m$ will be taken into account in further parts of this research work.

3.1. The precession moment

The gyroscopic precession moment results from the deflection of spin axis of an object while it is spinning. This moment causes a change in the orientation of the axis of rotation of the spinning object. The rotational axis will move about the original axis of rotation, making a circle called the precession circle. If a torque acts on a spinning body with direction perpendicular to plane that contains the axis of rotation and the angular momentum $\vec{L}$; the angular momentum changes from $\vec{L}$ to $\overrightarrow{dL}$ perpendicular to the vector $\vec{L}$ .The axis of rotation now points in the direction of sum of vectors, $\vec{L} + \overrightarrow{dL}$, having the same magnitude as $\vec{L}$ but pointing in a slightly different direction as shown in Fig. 6.

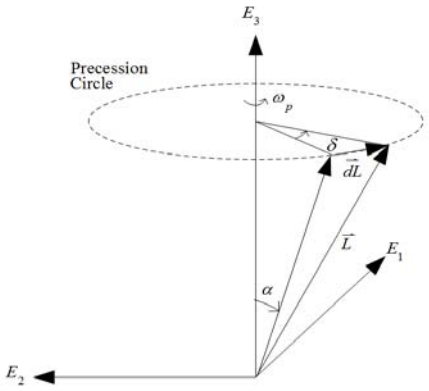

Fig. 6: The precession effect

The gyroscopic precession analysis can be applied to the tail rotor while it is tilting, as shown in Fig. 7.

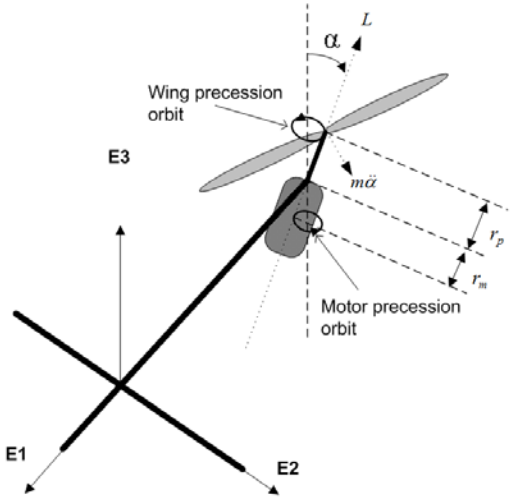

Fig. 7: The precession effect for the tail rotor

If m is the mass of the propeller, then the tail rotor tilting force $m\ddot{\alpha}$ produces a torque perpendicular to the angular momentum vector of the propeller. This causes a precession torque τ_{rp}, equal to the vector $\overrightarrow{dL}/dt$, in E_1E_2-plane, tangent to the precession circle in the Fig. 8.

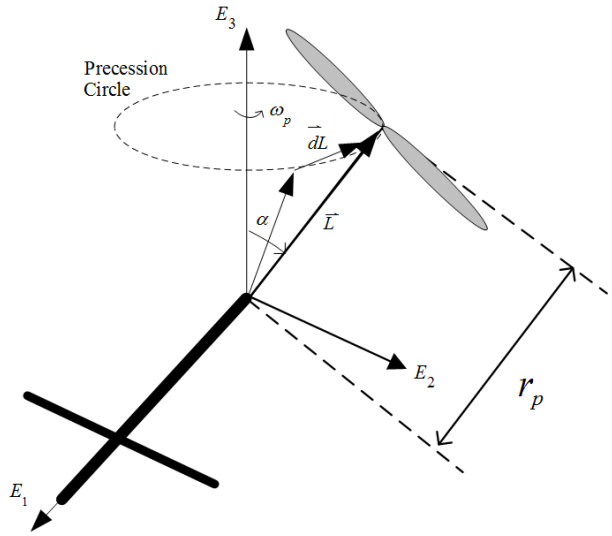

Fig. 8: The precession torque of the tail rotor propeller assembly

Since rotor is not free to inscribe the precession circle so precession moment effect gets added to the term ℵ in Eq. 1, in the yaw dynamics by Varignon's second moment theorem, so the precession moment vector is given by Eq. 3.

$$\mathrm{M_{pr}} = [0 \quad 0 \quad |\tau_{rp}|]^{\mathrm{T}} \tag{3}$$

3.2. The tilt rotor reaction moment

Consider a spinning body, with the velocity $\vec{\omega}$ and the moment of inertia I, undergoing an angular tilt with the rate $\vec{\Xi}$ as shown in Fig. 9.

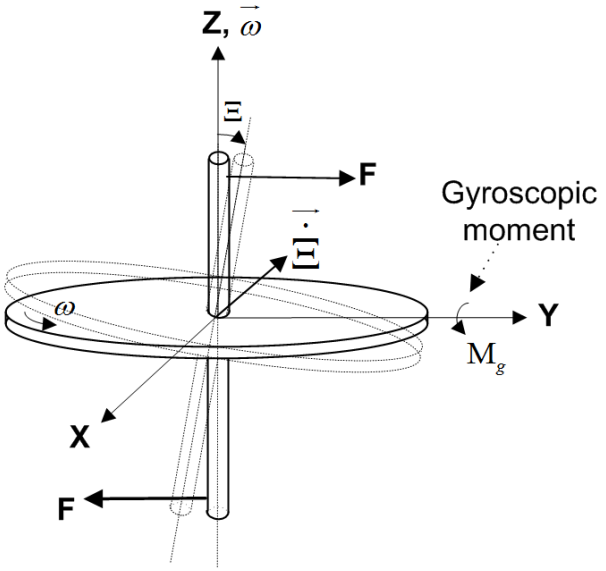

Fig. 9: The gyroscopic moment

Under these conditions the body experiences a gyroscopic moment given by Eq. 4.

$$M_g = \mathrm{I}\vec{\omega} \times \vec{\Xi} \tag{4}$$

In the case of the tail rotor that is tilting at a rate $\vec{\alpha}$, while rotating with a velocity $\vec{\omega}_3$, the gyroscopic moment M_{trg} is given by $\mathrm{I}\vec{\omega}_3 \times \vec{\alpha}$ and it is elaborated in Fig. 10. The plane of tail rotor tilt gyroscopic moment and its vector are also shown in Fig. 10. The tilt rotor gyroscopic moment has two orthogonal components in $E_2\,E_3$-plane, namely M_{trg2} and M_{trg3}. The tilt rotor gyroscopic moment vector that adds to ℵ in Eq. 1 is given by,

$$\mathrm{M_{trg}} = [0 \quad |M_{trg2}| \quad |M_{trg3}|]^{\mathrm{T}}$$
$$\text{or,} \qquad \mathrm{M_{trg}} = \begin{bmatrix} 0 \\ |M_{trg}|cos(\alpha) \\ |M_{trg}|sin(\alpha) \end{bmatrix} \tag{5}$$

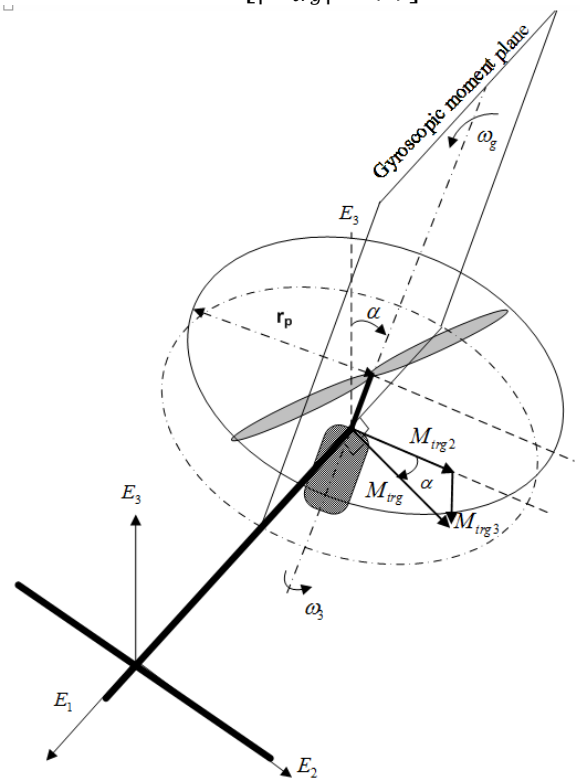

Fig. 10: Tail rotor tilts gyroscopic moment

3.3. The gyroscopic moment during roll

Consider a rigid body with "n" spinning bodies rigidly attached to it. Let the angular velocity of i^{th}spinning body be $\vec{\omega}_i$. Let moment of inertia of the body is I. If the body as a whole rotates with an angular velocity $\vec{\varrho}$ then the gyroscopic moment M_g experienced by the body is given by Eq. 6, which is an extension of Eq. 4.

$$M_g = \mathrm{I}\sum_{i=1}^{n} p\vec{\omega}_i \times \vec{\varrho}$$
$$p = \begin{cases} -1, & and for\ CCW\ rotation \\ 1, & and for\ CW\ rotation \end{cases} \tag{6}$$

Now considering the case of the T-copter body with three spinning propellers attached to it. Let the gyroscopic moment of i^{th} rotor during roll is denoted

by M_{gri}. Fig. 11 shows the scenario in which the T-Copter bodies under goes the roll manoeuvre. Using Eq. 4 the gyroscopic moments for rotor 2 and rotor 3 are shown in Figure 11. The rotor 1 is inclined at an angle α, so its angular velocity ω_1 is decomposed into the orthogonal components in E_2 E_3-plane, namely ω_{12} and ω_{13}. This vector resolution and the corresponding two gyroscopic moment components are shown in Fig. 12.

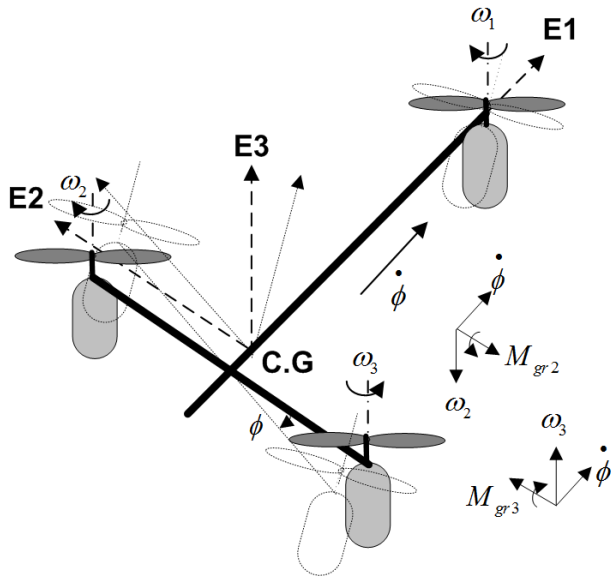

Fig. 11: Gyroscopic moments during roll

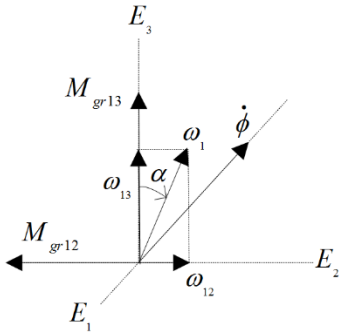

Fig. 12: Gyroscopic moment of tail rotor during roll

The net gyroscopic moment vector during roll is given by Eq. 7, by using Eq. 6 and the subsequent conversion to the η vector format.

$$\mathrm{M_{gr}} = \begin{bmatrix} 0 \\ |M_{gr3}| - |M_{gr2}| - |M_{gr13}| \\ |M_{gr13}| \end{bmatrix} \quad (7)$$

The individual components in Eq. 7 can be evaluated using Eq. 4. It is worth noting that $|M_{gr3}|$ and $|M_{gr2}|$ may cancel each other owing to the opposite direction of rotation of the main propellers if the rotors and the structure are perfectly symmetric and their speeds of rotation are equal. Any net imbalance may possibly be cancelled by $|M_{gr13}|$, which has adjustable magnitude by varying the angle α.

The moment of inertia terms for each individual gyroscopic component include the moment of inertia of the respective motor and propeller assembly. Let I_{mp} be the moment of inertia of motor-propeller assembly. Propeller and motor are approximated by parallelepiped and solid cylinder respectively, as shown in Fig. 13. The expression for I_{mp} is given by Eq. 8.

$$\mathrm{I}_{mp} = m_p \frac{l^2 + d^2}{12} + m_m r^2 \quad (8)$$

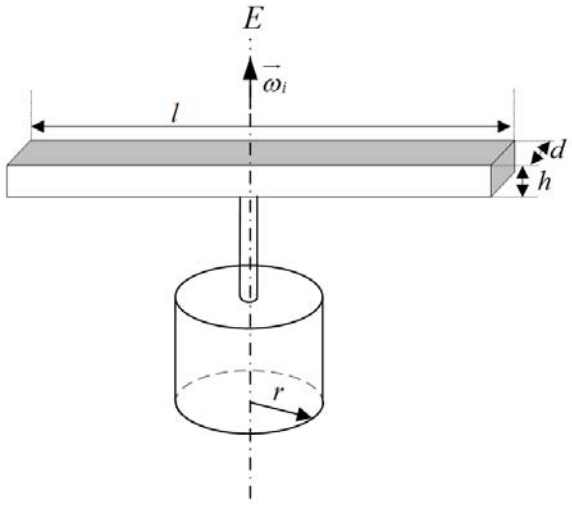

Fig. 13: Moment of inertia of motor-propeller set

3.4. The gyroscopic moments during pitch

Fig. 14 shows the scenario in which the T-Copter bodies under goes the pitch manoeuvre. Using Eq. 4 the gyroscopic moments for rotor 2 and rotor 3 are shown in Fig. 14. The rotor 1 is inclined at an angle α, so its angular velocity ω_1 is decomposed into the orthogonal components in E_2 E_3-plane, namely ω_{12} and ω_{13}. This vector resolution and the corresponding two gyroscopic moment components are shown in Fig. 15.

The net gyroscopic moment vector during pitch is given by Eq. 9, by using Eq. 6 and the subsequent conversion to the η vector format.

$$\mathrm{M_{gp}} = \begin{bmatrix} |M_{gp3}| + |M_{gp13}| - |M_{gp2}| \\ 0 \\ 0 \end{bmatrix} \quad (9)$$

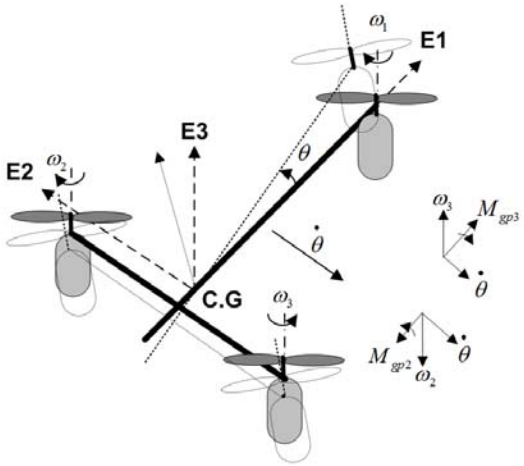

Fig. 14: Gyroscopic moments during pitch

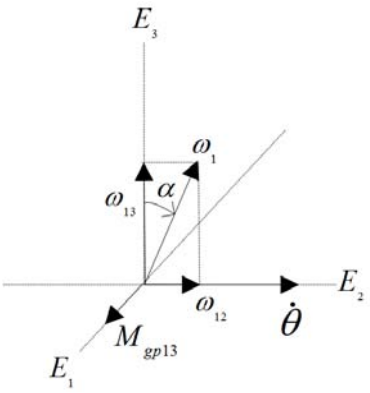

Fig. 15: Gyroscopic moment of tail rotor during pitch

The individual components in Eq. 9 can be evaluated using Eq. 4. The moment of inertia terms is the same as given by Eq. 8. It is worth noting that $|M_{gp3}|$ and $|M_{gp2}|$ may cancel each other owing to the opposite direction of rotation of the main propellers if the rotors and the structure are perfectly symmetric and their speeds of rotation are equal. Any net imbalance may possibly be cancelled by $|M_{gp13}|$, which has adjustable magnitude by varying the angle α.

3.5. The gyroscopic moments during yaw

Fig. 16 shows the scenario in which the T-Copter bodies under goes the yaw manoeuvre. Using the Eq. 4 the gyroscopic moments for rotor 2 and rotor 3 are shown in Fig. 16. The rotor 1 is inclined at an angle α, so its angular velocity ω_1 is decomposed into the orthogonal components in E_2 E_3-plane, namely ω_{12} and ω_{13}. This vector resolution and the corresponding two gyroscopic moment components are shown in Fig. 17. The net gyroscopic moment vector during yaw is given by Eq. 10, by using Eq. 5 and subsequent conversion to the η vector format.

$$\mathrm{M_{gy}} = \begin{bmatrix} -|M_{gy12}| \\ 0 \\ 0 \end{bmatrix} \qquad (10)$$

The individual components in Eq. 10 can be evaluated using Eq. 4. The moment of inertia terms is the same as given by Eq. 8.

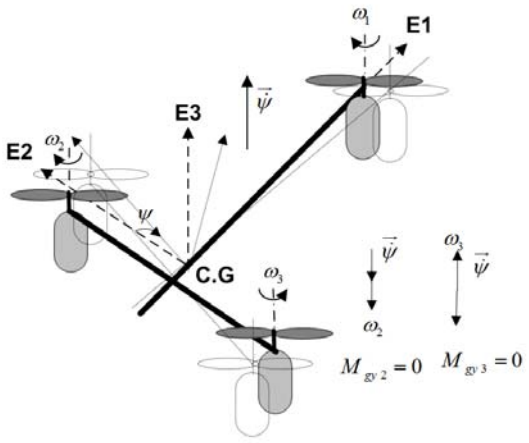

Fig. 16: Gyroscopic moments during yaw

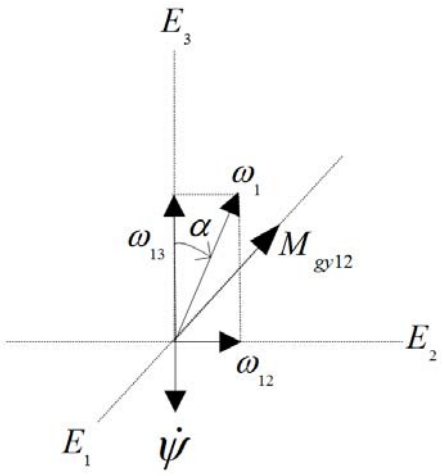

Fig. 17: Gyroscopic moment of tail rotor during yaw

3.6. The gyroscopic moments during tilt wing

As shown in Fig. 3, during tilting of the wing by servo mechanism, the main rotors rotate about E_2axis through an angle υ. The resulting gyroscopic moments are shown in Fig. 18.

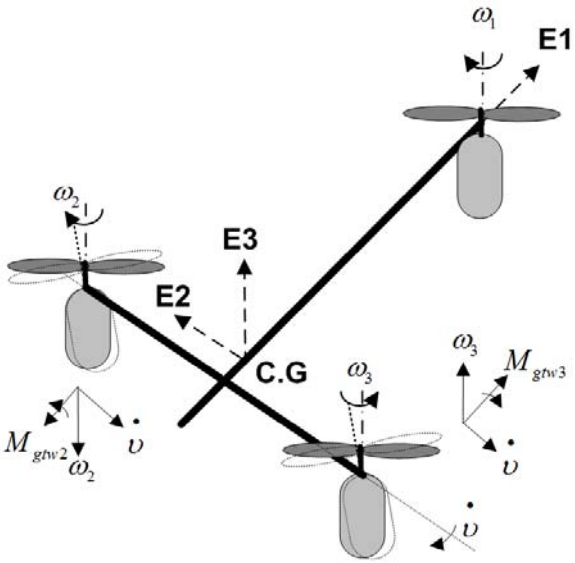

Fig. 18: Gyroscopic moments during tilt wing

The net gyroscopic moment vector during tilt wing is given by Eq. 11, by using Eq. 6 and the subsequent conversion to the η vector format.

$$\mathrm{M_{gtw}} = \begin{bmatrix} 0 \\ |M_{gtw3}| - |M_{gtw2}| \\ 0 \end{bmatrix} \qquad (11)$$

The individual components in Eq. 9 can be evaluated using Eq. 4. The moment of inertia terms is the same as given by Eq. 8. It is worth noting that $|M_{gtw3}|$ and $|M_{tw2}|$ may cancel each other owing to the opposite direction of rotation of the main propellers if the rotors and the structure are perfectly symmetric and their speeds of rotation are equal. Any net imbalance will get added to the roll dynamics of the system.

4. Dynamics equations including parasitics

The parasitic effects categorized in Eq. 2 can now be expressed by Eq. 12 and Eq. 13.

$$\aleph_p = M_{pr} \quad (12)$$

$$\aleph_g = M_{gr} + M_{gp} + M_{gy} + M_{trg} + M_{gtw} \quad (13)$$

The model in Eq. 1 modifies to Eq. 14, taking into account the effects modeled by Eq. 12 and Eq. 13.

$$I\frac{d^2\eta}{dt^2} = \tau + \{(M_{pr} + M_{gr} + M_{gp} + M_{gy} + M_{trg} + M_{gtw}) + \aleph_m\} \quad (14)$$

It is clear that model in Eq. 14 is not only nonlinear but also has cross coupling owing to the parasitic effects.

5. Discussion and conclusions

The dynamics of multi-rotor hybrid aircraft has been reviewed, taking into the account the terms that include the undesirable parasitic effects. Amongst various parasitic effects, the precession, and the gyroscopic effects have been studied and modeled in the detail in this part of the research paper. The developed equations have been elucidated and it has been shown that these terms are the major source of nonlinearity and cross coupling in the dynamics. The modeling and study of the remaining parasitic effects would be considered in the further parts of this research article.

References

Etkin B (1959). Dynamics of flight. John Wiley and Sons, Inc. New York, USA.

Goel R, Shah SM, Gupta NK and Ananthkrishnan N. (2009). Modeling, simulation and flight testing of an autonomous quadrotor. Proceedings of ICEAE, Indian Institute of Science, India: 1-7.

Haider A and Sajjad M (2012). Structural design and non-linear modeling of a highly stable multi-rotor hovercraft. Control Theory and Informatics, 2(4): 24-35.

Johnson W (2012). Helicopter theory. Courier Corporation. North Chelmsford, USA.

Kendoul F, Fantoni I and Lozano R (2005, December). Modeling and control of a small autonomous aircraft having two tilting rotors. InProceedings of the 44th IEEE Conference on Decision and Control, IEEE: 8144-8147.

Leishman JG (2006). Principles of Helicopter Aerodynamics. Cambridge University Press, Cambridge, UK.

Partovi AR, Xinhua W, Lum KY and Hai L (2011). Modeling and control of a small-scale hybrid aircraft. IFAC Proceedings Volumes, 44(1): 10385–10390

Salazar-Cruz S, Kendoul F, Lozano R and Fantoni I (2008). Real-time stabilization of a small three-rotor aircraft. IEEE Transactions on Aerospace and Electronic Systems, 44(2): 783-794.

Zhang W and Brandt RD (1999). Robust hovering control of PVTOL aircraft. IEE Transactions on Control Systems Technologies, 7(3): 343-351.